Characterization and Application of Nanomaterials 2025, 8(1), 10219.
https://doi.org/10.24294/can10219

Article

Enzymatic electrochemical biosensor for detection of L-Cysteine based on reduced graphene oxide modified glassy carbon electrode

Neeta Ukirade

Pratibha College of Commerce and Computer studies, Pune 411019, India; nitugatkal@gmail.com

CITATION

Ukirade N. Enzymatic electrochemical biosensor for detection of L-Cysteine based on reduced graphene oxide modified glassy carbon electrode. Characterization and Application of Nanomaterials. 2025; 8(1): 10219. https://doi.org/10.24294/can10219

ARTICLE INFO

Received: 23 December 2024
Accepted: 25 January 2025
Available online: 10 March 2025

Abstract: Cysteine is one of the body's essential amino acids to build proteins. For the early diagnosis of a number of diseases and biological issues, L-cysteine (L-Cys) is essential. Our study presents an electrochemical sensor that detects L-cysteine by immobilizing the horseradish peroxidase (HRP) enzyme on a reduced graphene oxide (GCE) modified glassy carbon electrode. The morphologies and chemical compositions of synthesized materials were examined using Fourier transform infrared spectroscopy (FTIR) and field-emission scanning electron microscopy (FESEM). The modified electrode's electrochemical behavior was investigated using cyclic voltammetry (CV). Cyclic voltammetry demonstrated HRP/rGO/GCE has better electrocatalytic activity than bare GCE in the oxidation of L-cysteine oxidation in a solution of acetate buffer. The electrochemical sensor had a broad linear range of 0 μM to 1 mM, a 0.32 μM detection limit, and a sensitivity of 6.08 μA μM^{-1} cm^{-2}. The developed sensor was successfully used for the L-cysteine detection in a real blood sample with good results.

Keywords: l-cysteine; enzyme; graphene oxide; electrochemical sensor; cyclic voltammetry

1. Introduction

The human body is composed of numerous biomolecules that are essential for various physiological functions. Biomolecules such as nucleic acids, carbohydrates, proteins, and amino acids are substances produced by living organisms and cells that perform a wide range of functions. Detection of the biomarkers associated with the diseases should be known and is possible by using biosensors. Cysteine (Cys) is an important amino acid used in the body and can also be taken as a supplement in the form of N-acetyl-L-cysteine. The detection of cysteine in biological samples has been the focus of numerous research efforts, as it plays an important role in many physiological processes [1]. Cys is often found in blood plasma in concentrations ranging from 53 to 300 mM, and it can be used as a key marker of health and disease risk. Cys insufficiency also causes skin lesions, hair depigmentation, edema, liver damage, muscle and fat loss, fatigue, and tiredness in addition to slower body growth. As a result, neurological pathogeneses, cystinosis, Parkinson's and Alzheimer's illnesses, and metabolic problems have all been linked to aberrant Cys accumulation and production. Therefore, developing rapid, low-cost, dependable, and sensitive analytical techniques to detect Cys would be crucial for protein quantification as well as for the early detection and prevention of neurological conditions, including Parkinson's and Alzheimer's illnesses as well as motor neuron disease [2]. To detect cysteine, various methods can be used, such as capillary electrophoresis (CE) [3], high-performance liquid chromatography (HPLC) [4], chemiluminescence [5], fluorescent probes [6], colorimetric [7], and electrochemical methods [8–10]. These

techniques allow for the sensitive as well as accurate detection of cysteine in biological samples. However, the aforementioned recognized methods are almost solely used in a rigorous lab environment, which is time demanding and requires a professional operator and expensive equipment [11,12]. Electrochemical techniques were recently thought to be the most practical because of their low cost, fast responsiveness, low detection limit, and great sensitivity [13,14].

Many studies on the electrochemical determination of Cys in various modified electrodes have been undertaken, for example, carbon-based electrodes [15–17], metal modified electrodes [18–20], polymer-modified electrodes [21,22]. Several electrochemical methods have been used to detect Cys. The electrochemical techniques used to detect Cys in an aqueous solution have been categorized based on the many electrical signals that Cys produces in the solution. Voltammetric techniques such as cyclic voltammetry (CV), differential pulse voltammetry (DPV), square wave voltammetry (SWV), linear sweep voltammetry (LSV), and others are highly suitable due to their high sensitivity, short analysis times, low level of detection (LOD), and low cost of equipment [23–25].

Furthermore, materials with enhanced surface conductivity were integrated into the sensor design to improve sensitivity and selectivity. Nanomaterial based electrochemical signal amplifications have enormous promise to improve both sensitivity and selectivity for electrochemical sensors and biosensors, with notable advancements in nanotechnology and nanoscience. In addition to metal nanoparticles, carbon-based materials (such as carbon nanotubes and graphene and its derivatives) have also gained a lot of attention in the development of electrochemical sensing platforms. This is primarily because of their advantageous properties, which include high surface area, excellent electrical conductivity, high mechanical strength, excellent performance and thermal stability [26,27].

Enzymes are large, intricate macromolecules that catalyze the rapid conversion of substrates into products; they are primarily composed of proteins. Enzyme-based electrochemical biosensors find extensive use in various fields such as healthcare, food safety, environmental monitoring. An enzyme-based biosensor uses the enzyme as the recognition element; to preserve enzyme activity, the enzyme is immobilized on or within the transducer surface's support matrix. Immobilized enzymes act as electrocatalysts, facilitating electron transfer between the electrode and the substrate molecule, leading to signal amplification and improved detection limits. Designing the biorecognition component of enzymatic biosensors requires careful consideration of the immobilization of enzymes. Numerous studies on enzyme immobilization methods, including entrapment, covalence, adsorption, affinity, and cross-linking, have been published [28–30].

In this study, we used an enzyme electrochemical biosensor based on Horseradish peroxidase to investigate electrochemical properties Cys. Firstly, we have synthesized rGO which was electrodeposited onto the bare GCE's surface. and horseradish peroxidase enzyme was then immobilized on the electrode surface using a gelatin membrane that was then cross-linked with glutaraldehyde. For the measurement of L-cysteine, the suggested sensor demonstrated great sensitivity, good biocompatibility, and a low detection limit. Graphene's huge specific surface area makes it an excellent substrate for providing a large number of catalytic active

sites. The designed electrode (Horseradish peroxidase/rGO/GCE) showed high selectivity for determination of Cys.

2. Materials and methods

2.1. Chemicals and apparatus

L-Cysteine, L-ascorbic acid, hydrochloride, dopamine, Nafion solution, uric acid and palladium (II) nitrate dihydrate phosphate buffer (PB) solution, Horseradish peroxidase, gluteraldehyde were purchased from Sigma-Aldrich (USA). Graphite powder potassium permanganate sulfuric acid (99.99%), hydrochloric acid, sodium nitrate, were purchased from Merck Company (Germany). All other compounds were analytical reagent grade and all solutions were made with double distilled water. The electrolyte used as the backdrop was phosphate buffer solution of 0.1 M (PBS, pH 7). A Potentiostat (CHI-1205B) was used for all of the cyclic voltammetry (CV) experiments. The frequency response analysis (FRA) module of a potentiostat was used to perform the electrochemical impedance spectroscopy (EIS) measurements. For the electrochemical measurements, a standard three-electrode cell assembly made up of a Pt wire counter electrode and an Ag/AgCl reference electrode was used. The working electrode was modified GCE.

2.2. Electrode preparation

The bare GC electrode was polished using alumina slurry at a thickness of 1, 0.3, and 0.05 μm respectively followed by washing with DI water, isopropanol, and finally sonication in DI water. Graphene oxide (GO) was synthesized by modified Hummer's method [31]. Furthermore, the synthesized GO reduced by annealing at 200, 300 and 400 ℃. After being thermally treated to become rGO powder, the dark brown powder turned to black [32]. Then 1 mg/mL of prepared rGO was dissolved in deionized water using an ultrasonicator. Subsequently, 5 μL rGO of the suspension was applied using the drop casting technique to the GCE surface, and it was allowed to dry for one hour at room temperature to produce the rGO modified GCE. In the next step, Horseradish peroxidase was immobilized onto rGO/GCE. This was accomplished by diluting 1 mg of horseradish peroxidase in 1 ml of phosphate buffer solution (pH 7.0). They then combined 12 mg of gelatin and 4 U of horseradish peroxidase in 100 μL of potassium phosphate buffer (pH 7.0) at 38 ℃ The modified electrode surface was then covered with 0.25μL of the mixed solution, which was let to dry for one hour at 4 ℃. Lastly, it was submerged for 5 min in a phosphate buffer (50 mM, pH 7.0) containing 2.5% glutaraldehyde to facilitate cross-linking. The films were further used to study electrochemical characteristics by voltammetry (CV).

3. Results and discussion

3.1. Characterization of HRP/rGO nanocomposite

3.1.1. Morphological studies

Surface morphology of the samples was observed by using field emission scanning electron microscopy (FESEM). **Figure 1** shows FESEM of **Figure 1a** rGO nanosheet and **Figure 1b** HRP/rGO surface. The result revealed that rGO exhibits a translucent, wrinkled-type, ultrathin, and flexible, sheet-like morphology. However, in case of rGO/GCE, a spherical like beads is spread over the surface as shown in **Figure 1b**. The result revealed that rGO proved to be an excellent carrier support for HRP immobilization.

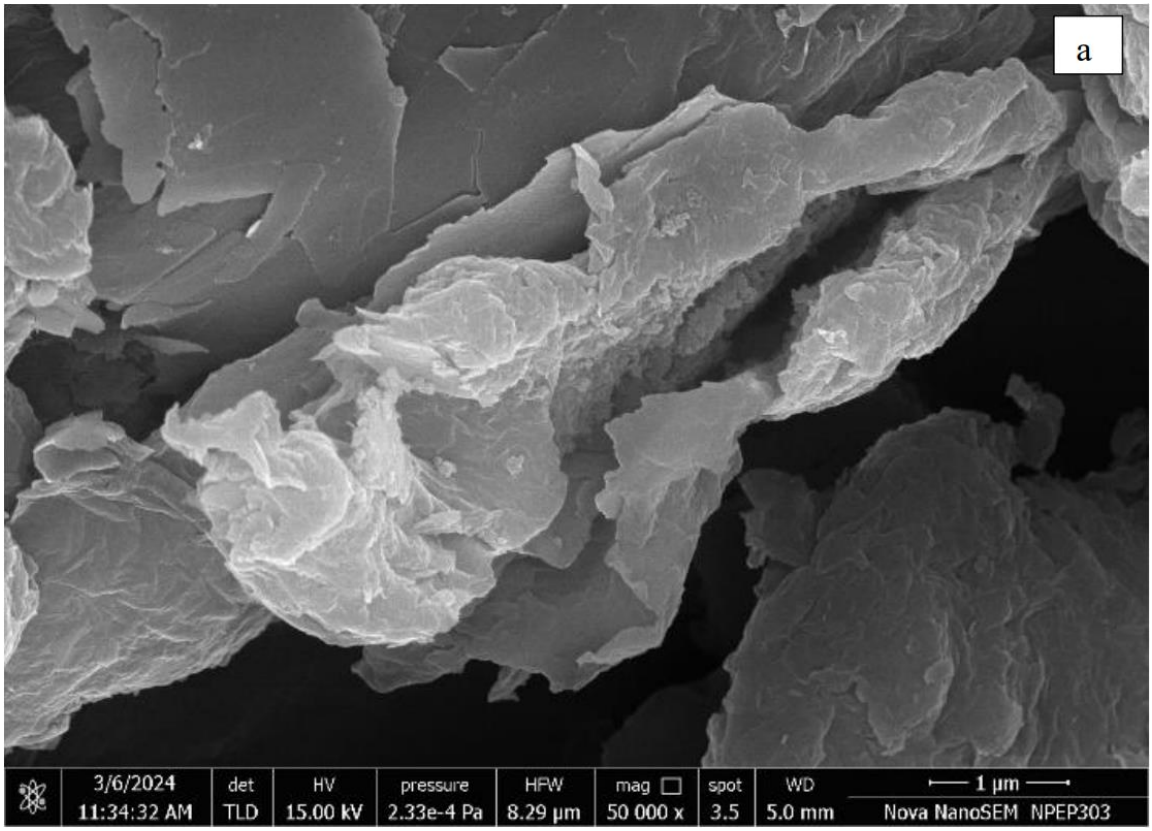

(a)

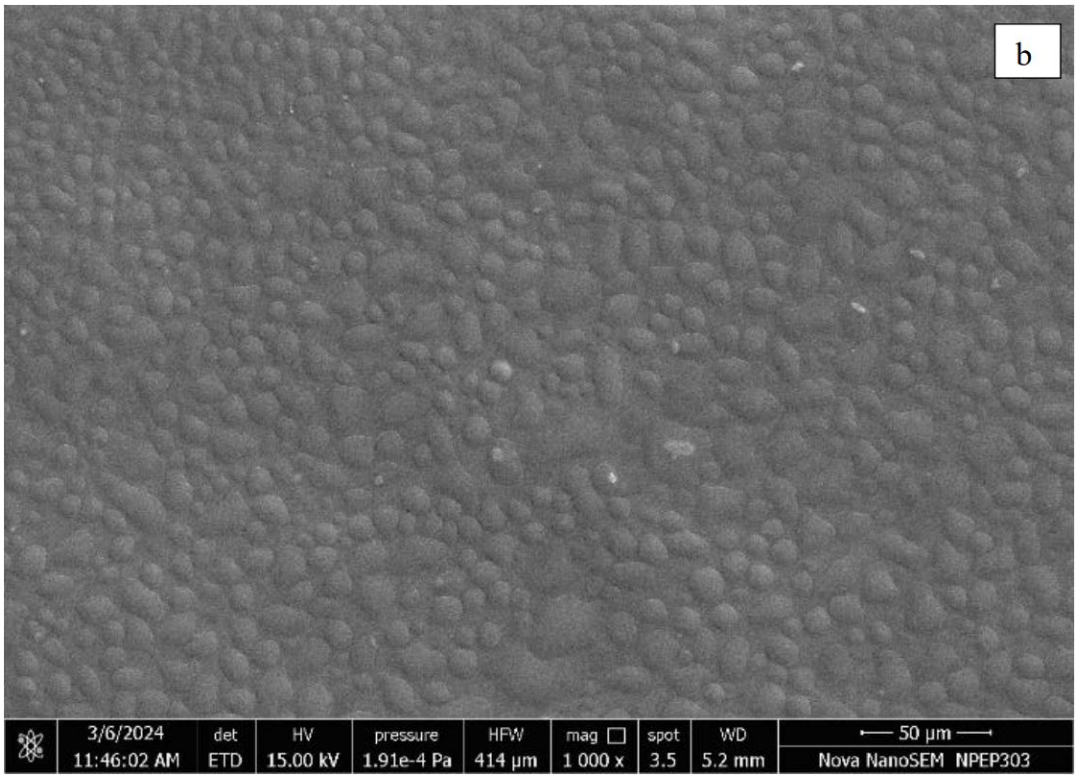

(b)

Figure 1. FESEM images of **(a)** rGO; **(b)** HRP/rGO.

3.1.2. Fourier transform infrared spectroscopy (FTIR)

Fourier-transform infrared spectroscopy (FTIR) is a potent analytical method which is commonly used to study the chemical composition and bonding of materials. **Figure 2** shows the FTIR spectra in the range from 4000 to 800 cm^{-1}). In the case of reduced graphene oxide (rGO), FTIR can provide information on the functional groups present on the rGO surface. The peaks visible at 3454 cm^{-1}, 1591 cm^{-1}, 1220 cm^{-1} corresponding to the O-H stretching, O-H stretching, C = O stretching, and C-O stretching vibration suggesting that the graphene was oxidised and the product rGO could be successfully dispersed in water. The alkyl (-CH2) chains' O-H vibration modes are responsible for the observed spectrum areas at 3380 cm^{-1} and 2920 cm^{-1}. Peaks at 1651 cm^{-1} assigned to the amide I, while aliphatic amines (C–N stretching vibration) assign at the region 1045 cm^{-1}. The FTIR spectrum of rGO-HRP showed that HRP was successfully immobilized onto rGO due to presence of characteristic peaks of HRP and the rGO.

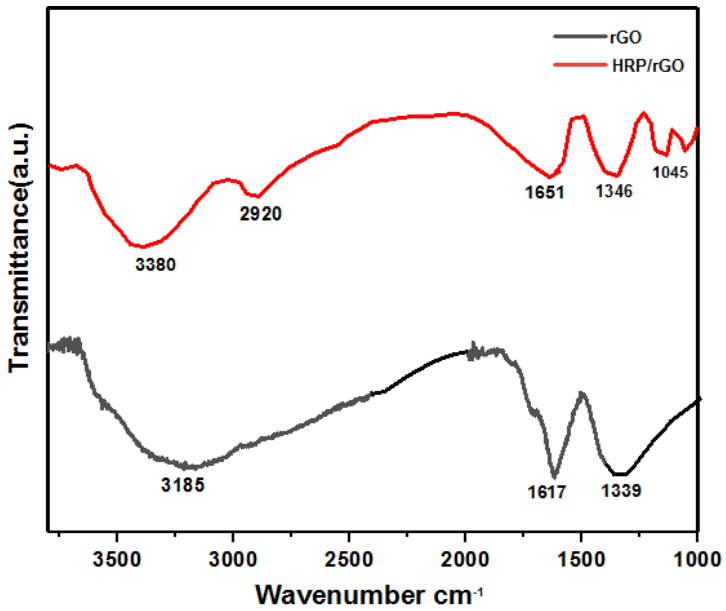

Figure 2. Fourier transform infrared spectroscopy (FTIR) spectra of rGO and HRP/rGO.

3.2. Electrochemical characterization of modified electrode

The electrochemical behavior of the various electrodes was examined by using CV at 40 mV scan rate in a 5 mM [Fe $(CN)_6]^{3-/4-}$ solution made in 0.1 M KCl solution. The chosen scanning speed for the cyclic voltammetry (CV) measurements was 40 mV/s. This value was selected based on a balance between achieving good signal resolution and maintaining reasonable experimental time. Cyclic Voltammograms (CVs) of bare GCE and modified GCE are shown in **Figure 3a** The CV of the bare GCE initially showed a 1:1 ratio between the anodic and cathodic peak currents and well-defined redox peaks showed related to the reversible redox behavior of [Fe $(CN)_6]^{3-/4-}$. After the modification of GCE with rGO, redox peak currents increase potentially as a result of semiconducting elements present. Additionally, compared to rGO/GCE electrode, the modified HRP/ rGO/GCE electrode showed significantly higher peak current, due to presence of HRP enzyme.

Electrochemical impedance spectroscopy (EIS) was used to examine the electron transfer properties of these electrodes. The electrode/electrolyte's electron-transfer resistance Rct is represented by the diameter of the semicircle in the EIS Nyquist plot. **Figure 3b** shows EIS of a) GCE, b) rGO/GCE, c) HRP/rGO/GCE in in 0.1 M KCl with 5 mM [Fe (CN)6]$^{3-/4-}$. The bare GCE exhibited a Ret of (310.5 Ω). A noticeable drop in resistance (267.6 Ω) was seen when the rGO was modified in the GCE. This was caused by the faster electron transport of Fe[(CN)6]$^{3-/4-}$ from the rGO to the electrode surface. However, the the modified electrode HRP/rGO/GCE had a lowest Ret of 89.2 Ω and hence it shows the highest conductivity.

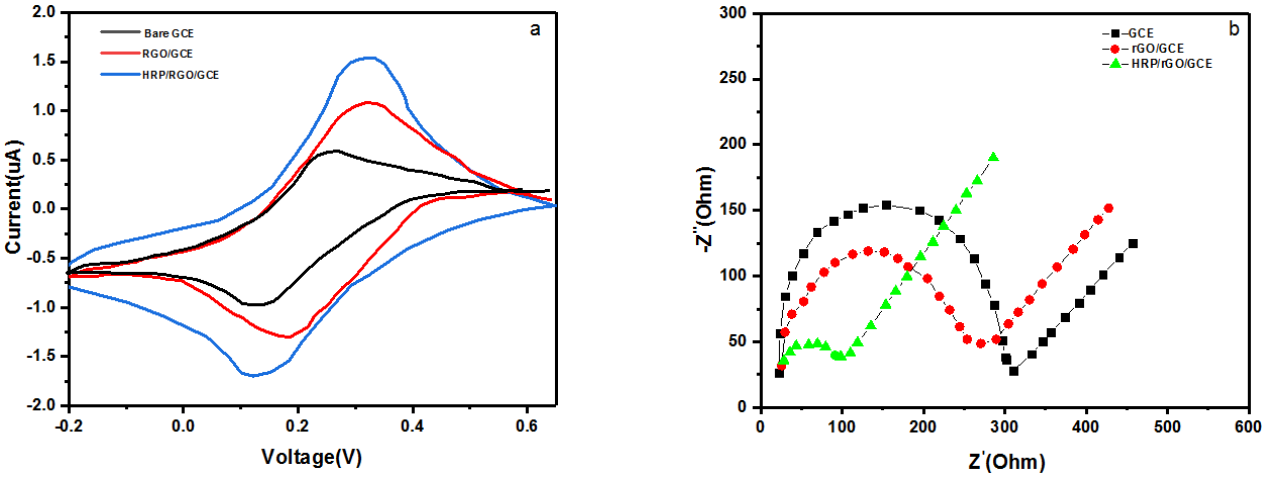

(a) **(b)**

Figure 3. (a) A cyclic voltammetry of modified electrodes in 0.1 M KCl containing 5 mM [Fe (CN)6]$^{3-/4-}$ at a scan rate 40 mV/s; **(b)** Nyquist plots for various modified electrodes in 0.1 M KCl with 5 mM [Fe $(CN)_6]^{3-/4-}$. Frequency range: 0.1 Hz to 10 Hz.

3.3. Effect of scan rate

To assess the behavior of L-Cys electrocatalytic oxidation on the HRP/rGO/GCE modified electrode, CVs were obtained at various scan rates using 0.1 M PB solution containing 200 µM L-Cys. The peak current density rises as the scan rate is increased from 10 to 100 mV.s^{-1}. as shown in **Figure 4**. There is a linear connection between the square root of the scan rate and the peak current density with R^2 = 0.9958. This suggests that the electrocatalytic oxidation of L-Cys is a diffusion-controlled electron transfer process on the modified electrode.

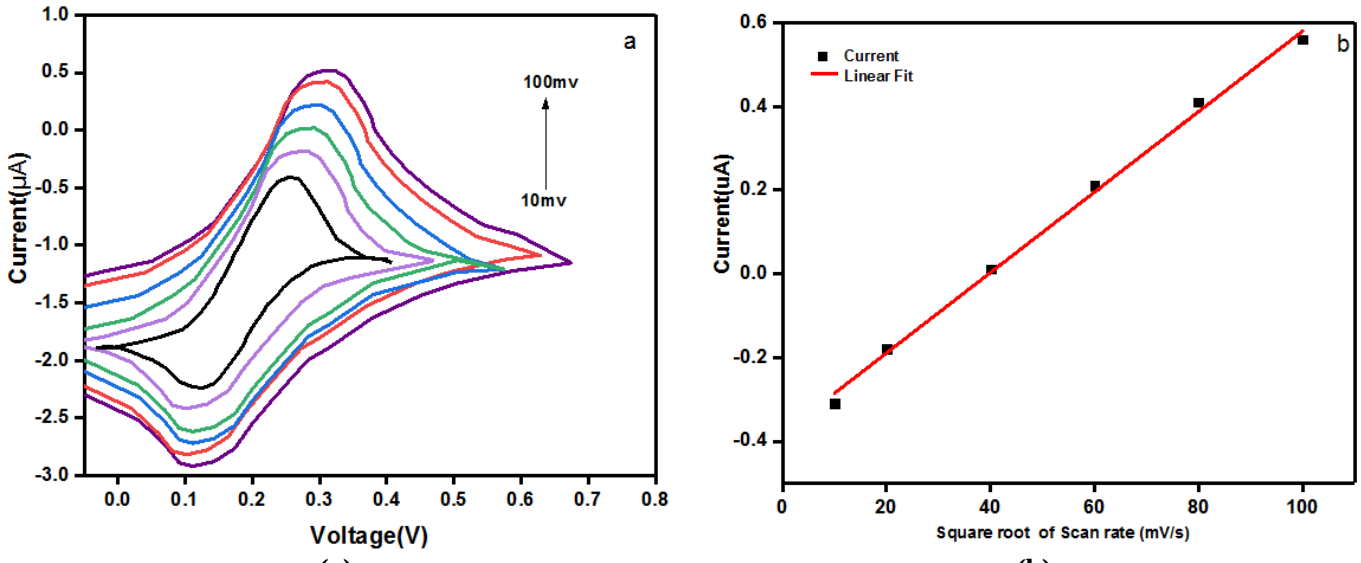

(a) **(b)**

Figure 4. (a) CV of the HRP/rGO/GCE under different scan rates (10 to 100 mVs^{-1}) in 0.5 mM Cys; **(b)** Relation between scan rate and peak current.

3.4. Electrocatalytic oxidation of L-cysteine

To assess the catalytic response of the HRP/rGO/GCE modified electrode to the oxidation of L-Cys, as shown in **Figure 5a**. A series of CV were recorded for various L-Cys concentrations. The results reveled that as the L-Cys concentration increases; current density also increases, providing more evidence of the electrode's electrocatalytic activity toward the oxidation of L-Cys. As seen in **Figure 5b**, the sensor shows high linearity in the concentration range of 0 µM to 1 mM with a correlation coefficient (R^2) of 0.9992. There is a linear relationship between the concentration of L-Cys and the current density of L-Cys. The sensor achieved a sensitivity of 6.08 $\mu A.\mu M^{-1}cm^{-2}$ with a LOD of 0.32 µM and quick response time demonstrates the HRP/rGO/GCE's promising catalytic activity toward L-Cys. For comparison, the detecting parameters based on different reported-nanomaterials with the proposed sensor in this study were listed in **Table 1.**

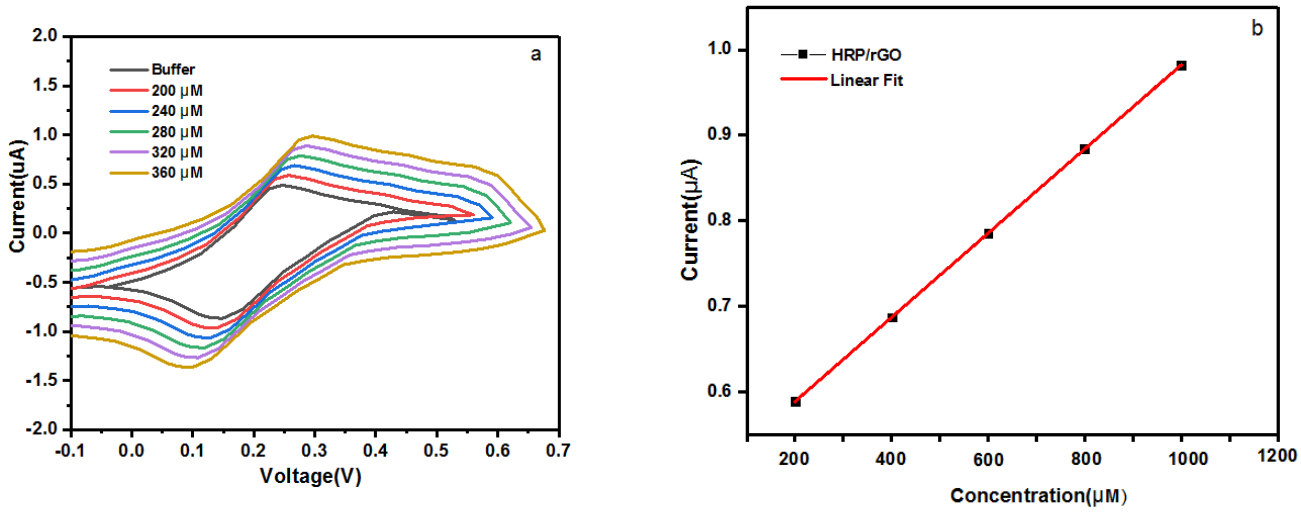

(a) **(b)**

Figure 5. (a) CV of a modified electrode scanning at a rate of 40 mVs^{-1} in a phosphate buffer with varying L-Cys concentrations**; (b)** Peak current against L-Cys concentration calibration plot 3.5.

3.5. Interference study

The applied voltage has a significant impact on the selectivity and sensitivity of the electrochemical sensors. **Figure 6** shows the electrochemical oxidation of 100 µM of various species AA, UA, DA, glucose and l-cysteine of 10 µM individually at pH 7.0 with a scan rate of 40 mVs^{-1} at different applied potentials by CV. The anodic peak is evidently the primary difference, since the catalytic current of L-cysteine oxidation peaked at the applied potential V, indicating that the applied voltage affects the sensor's selectivity. Almost no interference was observed in the presence of these foreign species. These findings indicated that AA, UA, DA, glucose did not significantly interfere with L-cysteine determination, and that this electrode has the potential to be employed for L-cysteine sensing in the presence of AA, UA, DA, glucose. These findings thus imply that the sensor electrode has outstanding selectivity for L-Cys detection. The reproducibility of the sensor was examined using four identical HRP/GO/GCE sensors. The CV responses to 10µM

L-Cys indicated no obvious current change among the four electrodes. The sensor's strong repeatability was confirmed by the 1.5% RSD value. CV from five successive measurements on a single electrode was used to assess repeatability, and the results were compared to the original value. After five iterations of measurements, the sensor maintains 94.2% of the original value. The electrode demonstrated 90% recovery with an RSD of 4.03% for LCys detection after 8 days, indicating the sensor's strong stability.

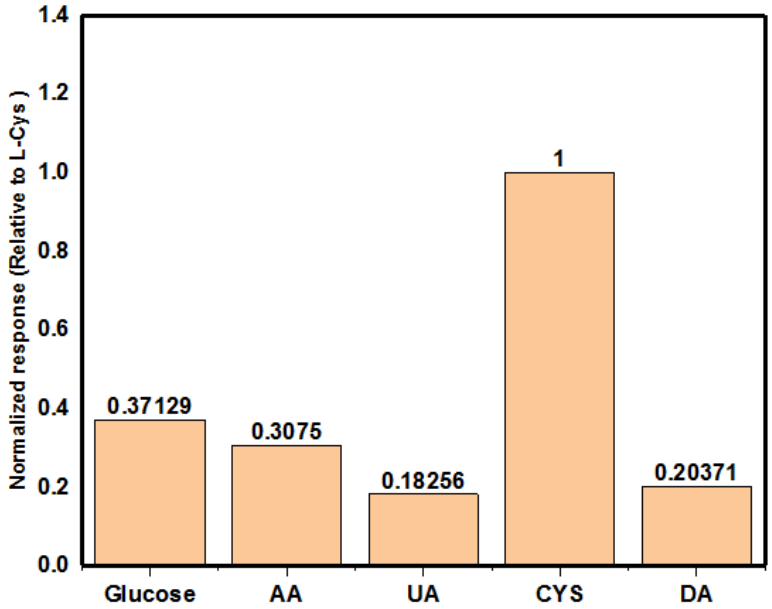

Figure 6. The electrochemical oxidation of 100 µM of some species (AA, UA, DA, glucose and l-cysteine) at pH 7.0 with scan rate 40 mV/s by CV technique.

Table 1. Comparison of the analytical performance of HRP/GO/GCE sensor with some carbon-based earlier sensors for the detection of Cys.

Sr. No	Modified electrodes	Linear range (µM)	Limit of Detection (µM)	References
1	CuFe2O4/rGO–Au	50–200; 0–15,000	0.383; 0.598	[33]
2	20%Pd@Ti3C2Tx/GCE	0.5–10	0.14	[34]
3	Pt-Fe3O4-rGO/GCE	100–1000	10.1	[35]
4	CoHCF/GCE	6–1000 1.5–200	4	[36]
5	rGO-Nafion@Pd6/GCE	0.5–10	0.15	[37]
6	AuNR/MWCNT/GCE	5–200	0.008	[38]
7	HRP /rGO/GCE	0–1000	0.32	This work

4. Conclusions

The electroanalytical measurement of Cysteine was carried out using Horseradish peroxidase (HRP) enzyme immobilized on a modified glassy carbon electrode (GCE) using graphene oxide where electrocatalytic oxidation was observed to occur at a lower overpotential when compared to bare GCE. This sensor apparatus offered a quick response, a good LOD, and great selectivity. In addition, the sensor demonstrated good reproducibility, repeatability, and stability. Lastly, the

modified sensor showed intriguing analytical features, including larger detection ranges between 0 and 1 mM, a noteworthy LOD of 0.32 μM, and super electrocatalytic activities. It has a few additional advantages, such as ease of manufacture, better electrocatalysis, and efficient discrimination from typical interfering bimolecular compounds with rapid and stable response to Cysteine.

Acknowledgments: Neeta Ukirade is grateful to Pratibha College of Commerce and Computer Studies, Chinchwad, for providing the facility to carry out the research work.

Conflict of interest: The author declares no conflict of interest.

References

1. Rehman T, Shabbir MA, Inam-Ur-Raheem M, et al. Cysteine and homocysteine as biomarker of various diseases. Food Science & Nutrition. 2020; 8(9): 4696–4707. doi: 10.1002/fsn3.1818
2. Tajik S, Dourandish Z, Jahani PM, et al. Recent developments in voltammetric and amperometric sensors for cysteine detection. RSC Advances. 2021; 11(10): 5411–5425. doi: 10.1039/d0ra07614g
3. Ivanov AV, Bulgakova PO, Virus ED, et al. Capillary electrophoresis coupled with chloroform-acetonitrile extraction for rapid and highly selective determination of cysteine and homocysteine levels in human blood plasma and urine. ELECTROPHORESIS. 2017; 38(20): 2646–2653. doi: 10.1002/elps.201700133
4. Forgacsova A, Galba J, Mojzisova J, et al. Ultra-high performance hydrophilic interaction liquid chromatography—Triple quadrupole tandem mass spectrometry method for determination of cysteine, homocysteine, cysteinyl-glycine and glutathione in rat plasma. Journal of Pharmaceutical and Biomedical Analysis. 2019; 164: 442–451. doi: 10.1016/j.jpba.2018.10.053
5. Yang N, Song H, Wan X, et al. A metal (Co)–organic framework-based chemiluminescence system for selective detection of l-cysteine. The Analyst. 2015; 140(8): 2656–2663. doi: 10.1039/c5an00022j
6. Zhang L, Lu B, Lu C, et al. Determination of cysteine, homocysteine, cystine, and homocystine in biological fluids by HPLC using fluorosurfactant-capped gold nanoparticles as postcolumn colorimetric reagents. Journal of Separation Science. 2013; 37(1–2): 30–36. doi: 10.1002/jssc.201300998
7. Hai X, Lin X, Chen X, et al. Highly selective and sensitive detection of cysteine with a graphene quantum dots-gold nanoparticles based core-shell nanosensor. Sensors and Actuators B: Chemical. 2018; 257: 228–236. doi: 10.1016/j.snb.2017.10.169
8. Kazemi S, Karimi-Maleh H, Hosseinzadeh R, et al. Selective and sensitive voltammetric sensor based on modified multiwall carbon nanotubes paste electrode for simultaneous determination of l-cysteine and folic acid. Ionics. 2012; 19(6): 933–940. doi: 10.1007/s11581-012-0816-7
9. Jerome R, Keerthivasan PV, Murugan N, et al. Preparation of Stable CuO/Boron Nitride Nanocomposite Modified Electrode for Selective Electrochemical Detection of L–Cysteine. ChemistrySelect. 2020; 5(29): 9111–9118. doi: 10.1002/slct.202002105
10. Thota R, Ganesh V. Simple and facile preparation of silver–polydopamine (Ag–PDA) core–shell nanoparticles for selective electrochemical detection of cysteine. RSC Advances. 2016; 6(55): 49578–49587. doi: 10.1039/c6ra06994k
11. Cao F, Huang Y, Wang F, et al. A high-performance electrochemical sensor for biologically meaningful l-cysteine based on a new nanostructured l-cysteine electrocatalyst. Analytica Chimica Acta. 2018; 1019: 103–110. doi: 10.1016/j.aca.2018.02.048
12. Majd SM, Teymourian H, Salimi A. Fabrication of an Electrochemical L-Cysteine Sensor Based on Graphene Nanosheets Decorated Manganese Oxide Nanocomposite Modified Glassy Carbon Electrode. Electroanalysis. 2013; 25(9): 2201–2210. doi: 10.1002/elan.201300245
13. Perevezentseva DO, Gorchakov EV. Voltammetric determination of cysteine at a graphite electrode modified with gold nanoparticles. Journal of Solid State Electrochemistry. 2012; 16(7): 2405–2410. doi: 10.1007/s10008-012-1727-2

14. Liu X, Luo L, Ding Y, et al. Simultaneous determination of L-cysteine and L-tyrosine using Au-nanoparticles/poly-eriochrome black T film modified glassy carbon electrode. Bioelectrochemistry. 2012; 86: 38–45. doi: 10.1016/j.bioelechem.2012.01.008
15. Yang S, Li G, Wang Y, et al. Amperometric L-cysteine sensor based on a carbon paste electrode modified with Y2O3 nanoparticles supported on nitrogen-doped reduced graphene oxide. Microchimica Acta. 2016; 183(4): 1351–1357. doi: 10.1007/s00604-015-1737-8
16. Al-Gahouari T, Bodkhe G, Sayyad P, et al. Electrochemical sensor: L-cysteine induced selectivity enhancement of electrochemically reduced graphene oxide–multiwalled carbon nanotubes hybrid for detection of lead (Pb 2+) ions. Frontiers in Materials. 2020; 7: 68. doi: 10.3389/fmats.2020.00068
17. Singh M, Jaiswal N, Tiwari I, et al. A reduced graphene oxide-cyclodextrin-platinum nanocomposite modified screen printed electrode for the detection of cysteine. Journal of Electroanalytical Chemistry. 2018; 829: 230–240. doi: 10.1016/j.jelechem.2018.09.018
18. Li J, Zhang L. 3D pothole-rich hierarchical carbon framework-encapsulated Ni nanoparticles for highly selective nonenzymatic cysteine detection. Electrochimica Acta. 2019; 328: 135126. doi: 10.1016/j.electacta.2019.135126
19. Kaur B, Srivastava R, Satpati B. A novel gold nanoparticle decorated nanocrystalline zeolite based electrochemical sensor for the nanomolar simultaneous detection of cysteine and glutathione. RSC Advances. 2015; 5(115): 95028–95037. doi: 10.1039/c5ra19249h
20. Wu L, Li J, Zhang H. One Step Fabrication of Au Nanoparticles-Ni-Al Layered Double Hydroxide Composite Film for the Determination of L-Cysteine. Electroanalysis. 2015; 27(5): 1195–1201. doi: 10.1002/elan.201400624
21. Ziyatdinova G, Kozlova E, Budnikov H. Selective electrochemical sensor based on the electropolymerized p-coumaric acid for the direct determination of l-cysteine. Electrochimica Acta. 2018; 270: 369–377. doi: 10.1016/j.electacta.2018.03.102
22. Ojani R, Raoof JB, Zarei E. Preparation of poly N, N-dimethylaniline/ferrocyanide film modified carbon paste electrode: Application to electrocatalytic oxidation of l-cysteine. Journal of Electroanalytical Chemistry. 2010; 638(2): 241–245. doi: 10.1016/j.jelechem.2009.11.005
23. Moradi R, Sebt SA, Karimi-Maleh H, et al. Synthesis and application of FePt/CNTs nanocomposite as a sensor and novel amide ligand as a mediator for simultaneous determination of glutathione, nicotinamide adenine dinucleotide and tryptophan. Physical Chemistry Chemical Physics. 2013; 15(16): 5888–5897. doi: 10.1039/c3cp00033h
24. Ru J, Du J, Qin DD, et al. An electrochemical glutathione biosensor: Ubiquinone as a transducer. Talanta. 2013; 110: 15–20. doi: 10.1016/j.talanta.2013.03.038
25. Malik S, Singh J, Goyat R, et al. Nanomaterials-based biosensor and their applications: A review. Heliyon. 2023; 9(9): e19929. doi: 10.1016/j.heliyon.2023.e19929
26. Suhito IR, Koo KM, Kim TH. Recent Advances in Electrochemical Sensors for the Detection of Biomolecules and Whole Cells. Biomedicines. 2020; 9(1): 15. doi: 10.3390/biomedicines9010015
27. Kilic NM, Singh S, Keles G, et al. Novel Approaches to Enzyme-Based Electrochemical Nanobiosensors. Biosensors. 2023; 13(6): 622. doi: 10.3390/bios13060622
28. Fredj Z, Singh B, Bahri M, et al. Enzymatic Electrochemical Biosensors for Neurotransmitters Detection: Recent Achievements and Trends. Chemosensors. 2023; 11(7): 388. doi: 10.3390/chemosensors11070388
29. Navaee A, Salimi A. Enzyme-based electrochemical biosensors. Electrochemical Biosensors. 2019: 167–211. doi: 10.1016/b978-0-12-816491-4.00007-3
30. Hummers WS, Offeman RE. Preparation of Graphitic Oxide. Journal of the American Chemical Society. 1958; 80(6): 1339–1339. doi: 10.1021/ja01539a017
31. Hidayat R, Wahyuningsih S, Ramelan A. Simple synthesis of rGO (reduced graphene oxide) by thermal reduction of GO (graphene oxide). IOP Conference Series: Materials Science and Engineering. 2020; 858(1): 012009. doi: 10.1088/1757-899x/858/1/012009
32. Atacan K. CuFe2O4/reduced graphene oxide nanocomposite decorated with gold nanoparticles as a new electrochemical sensor material for L-cysteine detection. Journal of Alloys and Compounds. 2019; 791: 391–401. doi: 10.1016/j.jallcom.2019.03.303
33. Rasheed PA, Pandey RP, Jabbar KA, et al. Sensitive electrochemical detection of l-cysteine based on a highly stable Pd@Ti3C2Tx (MXene) nanocomposite modified glassy carbon electrode. Analytical Methods. 2019; 11(30): 3851–3856. doi: 10.1039/c9ay00912d

34. Wang Y, Wang W, Li G, et al. Electrochemical detection of L-cysteine using a glassy carbon electrode modified with a two-dimensional composite prepared from platinum and Fe3O4 nanoparticles on reduced graphene oxide. Microchimica Acta. 2016; 183(12): 3221–3228. doi: 10.1007/s00604-016-1974-5
35. Abbaspour A, Ghaffarinejad A. Electrocatalytic oxidation of l-cysteine with a stable copper–cobalt hexacyanoferrate electrochemically modified carbon paste electrode. Electrochimica Acta. 2008; 53(22): 6643–6650. doi: 10.1016/j.electacta.2008.04.065
36. Yusoff N, Rameshkumar P, Mohamed Noor A, et al. Amperometric determination of L-cysteine using a glassy carbon electrode modified with palladium nanoparticles grown on reduced graphene oxide in a Nafion matrix. Microchimica Acta. 2018; 185(4): 1–10. doi: 10.1007/s00604-018-2782-x
37. Silva F de A dos S, da Silva MGA, Lima PR, et al. A very low potential electrochemical detection of l-cysteine based on a glassy carbon electrode modified with multi-walled carbon nanotubes/gold nanorods. Biosensors and Bioelectronics. 2013; 50: 202–209. doi: 10.1016/j.bios.2013.06.036
38. Sui M, Huang Y, Tang Y, et al. A high-sensitivity AuNPs/MWCNTs-MB/DNA-GCE quadruplex biosensor for Pb detection in medicinal teas through in-situ monitoring microstructure and conformational switch by SECM. Sensors and Actuators B: Chemical. 2023; 393: 134193. doi: 10.1016/j.snb.2023.134193